

Mechanism of Fermi acceleration in dispersing billiards with time-dependent boundaries

A. Yu. Loskutov,^{*} A. B. Ryabov, and L. G. Akinshin

M. V. Lomonosov Moscow State University, 119899 Moscow, Russia

(Submitted 17 February 1999)

Zh. Éksp. Teor. Fiz. **116**, 1781–1797 (November 1999)

The paper is devoted to the problem of Fermi acceleration in Lorentz-type dispersing billiards whose boundaries depend on time in a certain way. Two cases of boundary oscillations are considered: the stochastic case, when a boundary changes following a random function, and a regular case with a boundary varied according to a harmonic law. Analytic calculations show that the Fermi acceleration takes place in such systems. The first and second moments of the velocity increment of a billiard particle, alongside the mean velocity in a particle ensemble as a function of time and number of collisions, have been investigated. Velocity distributions of particles have been obtained. Analytic and numerical calculations have been compared. © 1999 American Institute of Physics. [S1063-7761(99)02111-3]

1. INTRODUCTION

The term *billiard* is applied to a dynamic system in which a point-like particle moves within a certain region Q with a piecewise smooth boundary ∂Q under the condition that the law of equality between the angles of incidence and reflection applies. Depending on the billiard boundary configuration, the motion of the particle (billiard ball) can be regular, ergodic, or mixing. The term *dispersing billiard*¹ applies to a system whose boundary ∂Q is convex inside the region Q . It is well known that such a billiard has a mixing property, and the billiard ball dynamics in this case is chaotic.

If the set ∂Q is constant with time, the system is called a billiard with a constant (fixed) boundary, but if $\partial Q = \partial Q(t)$, this is a billiard with a perturbed (moving) boundary. Billiards with fixed boundaries have been well studied (see Refs. 1–7 and references therein). At the same time, there have been very few publications devoted to billiards with perturbed boundaries,^{7–11} although their studies are of great interest from the viewpoints of both solutions of some problems of statistical mechanics and the feasibility of an unbounded increase in a ball velocity, the latter problem originating from that of the so-called Fermi acceleration.^{12,13}

Fermi acceleration is the phenomenon of infinite acceleration of particles of various nature owing to their scattering by moving massive scatterers. This mechanism of acceleration was first suggested by Fermi¹² to account for the origin of cosmic rays of very high energies. Later various models were suggested,^{14–21} which described this phenomenon with a lesser or greater degree of success. For example, Ulam¹⁴ demonstrated that, if a particle moves between an oscillating and a fixed wall, and the oscillation phase of the former at the moment of collision is a random value, the particle can acquire an infinitely high velocity. A more detailed investigation of Ulam's model was conducted by Lieberman and Lichtenberg,¹⁶ who showed that, in the case of a smooth time

dependence of the wall velocity, stochastic layers are separated by invariant curves. These curves set limits on the energy acquired by the particle. If this dependence is not sufficiently smooth, there are no invariant curves, and the particle velocity can increase without bound. Later investigations (see Refs. 16,19–21 and references therein) of various versions of Ulam's model revealed some relation between the law governing wall oscillations (i.e., the smoothness of the wall velocity as a function of time and the degree of its randomness) and the presence of the Fermi acceleration.

In chaotic billiards, even if the boundary velocity is a smooth function of time, the incidence angle of a particle can be treated as a random parameter. Consequently, the normal velocity component at the collision point (this is the component that changes as a result of scattering, whereas the tangential component is constant) is a stochastic value. Obviously, changes in the velocity are also random in this case.

The paper is devoted to the problem of Fermi acceleration treated on the example of a generalized billiard, namely, a Lorentz gas with an open horizon and a perturbed boundary. We focus attention on two different cases of stochastic and regular (harmonic) oscillations of the boundary. Note that in all publications on this topic of which we are aware, the problem of Fermi acceleration was investigated in integrable or almost integrable systems. In view of this, our paper presents the first investigation of chaotic billiards with perturbed boundaries.

The paper comprises three main sections. The first of them is devoted to the basic concepts and derivation of maps that describe the dynamics of a billiard. The second describes the analytic and numerical study of the feasibility of Fermi acceleration. The third presents numerical calculations of the particle velocity as a function of time and number of scattering events, and compares them to analytic results.

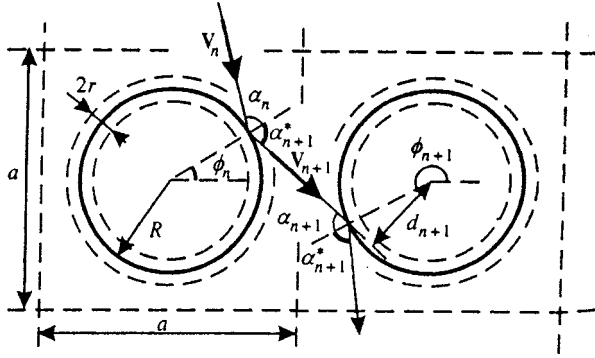


FIG. 1. Configuration of Lorentz gas model. The scatterers (circles of radius R) are located at sites of a periodic lattice with period a .

2. LORENTZ GAS

This section is devoted to the main concepts and derivation of mappings that determine the dynamics of a two-dimensional Lorentz gas.

Consider a plane area Q with a piecewise smooth boundary ∂Q . The dispersing billiard^{1,4} is a system composed of neutral ∂Q_i^0 and dispersing ∂Q_i^+ (i.e., convex in the region Q) sections of the boundary ∂Q . One representative of such billiards is a system defined in an unbounded domain D and composed of a set of round infinitely heavy scatterers B_i with boundaries ∂Q_i and of radii R located at sites of an infinite periodic lattice with period a (Fig. 1). Given that B_i are fixed, the billiard in the region $Q = D \setminus \cup_{i=1}^{\infty} B_i$ is called a Lorentz gas. A particle moves among the scatterers and reflects from them in accordance with the mirror reflection law. Such a billiard has been studied in detail in the case of $\partial Q = \text{const}$ (see Refs. 1, 3, 4, 6 and references therein).

The ratio $(a/R)^2$ is one of the main parameters of the Lorentz gas. Depending on this parameter, we distinguish Lorentz gases with a bounded horizon [$(a/R)^2 < 4$], with an open horizon [$4 < (a/R)^2 < 8$], and with an infinite horizon [$(a/R)^2 > 8$]. In the first case, the particle motion is limited to one lattice cell, in the second and third cases it can travel throughout the entire space. In the case of an infinite horizon, statistical properties of a billiard change because of higher probabilities of long free paths,^{3,4,22-24} whereas in Lorentz gases with bounded and open horizons correlations decay exponentially. The mean free path is defined as $l = \pi A/P$, where A is the area of a billiard where a particle can go and P is the scatterer perimeter. For a system with an open horizon $l = (a^2 - \pi R^2)/2R$, and for a billiard with an infinite horizon l has no upper bound.

Suppose that the radii of scatterers B_i in a Lorentz gas are perturbed in accordance with a certain law, i.e., all boundaries ∂Q_i perform small oscillations in the normal direction. In this paper we consider two different cases: periodic (and phase-synchronized) oscillations, and random changes in scatterer radii. The first case corresponds to the situation when all boundaries oscillate in phase following the same law. The second case describes oscillations of many scatterer boundaries with the initial phases distributed randomly.

2.1. Lorentz gas with a fixed boundary

It is known that one can select as canonical variables for billiards with unperturbed boundaries the azimuthal angle ϕ and incidence angle α between the interior normal to the surface and particle velocity before the collision. Let us introduce the reflection angle α^* between the exterior normal and velocity after the collision (Fig. 1). It is obvious that $\phi \in [0, 2\pi]$, and the angles α and α^* vary over the interval $[-\pi/2, \pi/2]$. In order to describe the dynamics of an unperturbed billiard, one has to calculate a mapping $(\alpha_n, \phi_n) \rightarrow (\alpha_{n+1}, \phi_{n+1})$ which transforms the variables (α, ϕ) at the moment before the n th collision with ∂Q to their values at the moment before the $(n+1)$ th collision. It clearly follows from geometrical considerations (Fig. 1) that

$$\phi_n + \alpha_n^* + \pi = \phi_{n+1} + \alpha_{n+1}. \tag{1}$$

Moreover, $\alpha_n^* = -\alpha_n$ since these angles are measured in opposite directions.

Let us introduce a reference frame with its origin at the center of a circle on which the latest scattering event has taken place and determine the equation of the straight line along which the particle travels after the collision. Then one can easily calculate the distance at which the particle passes another center at a distance of p cells along the horizontal axis and q cell along the vertical axis:

$$d_{n+1} = a[p \sin(\phi_n + \alpha_n^*) - q \cos(\phi_n + \alpha_n^*)] - R \sin \alpha_n^*. \tag{2}$$

The parameter p is assumed to be positive if the particle moves on the right of the center and negative if the particle moves on the left. Accordingly, q is positive if the particle moves upwards and negative if it moves downwards. The values p and q are determined using the scattering condition, i.e., these are integers with the smallest absolute values at which the condition $|d_{n+1}| \leq R$ is satisfied. After calculating the impact parameter d_{n+1} , one can easily calculate the angle at which the collision with the next scatterer will take place:

$$\alpha_{n+1} = \sin^{-1} \frac{d_{n+1}}{R}. \tag{3}$$

The Jacobian of the resulting mapping defined by Eqs. (1)–(3) is

$$\frac{\partial(\phi_{n+1}, \alpha_{n+1})}{\partial(\phi_n, \alpha_n)} = \frac{\cos \alpha_n}{\cos \alpha_{n+1}}.$$

Thus, the mapping preserves the phase volume $\cos \alpha d\alpha d\phi$. Hence follows, in particular, that if the billiard is ergodic, the distribution with respect to α_n is described by the formula

$$\rho_\alpha(\alpha) = \frac{1}{2} \cos \alpha, \tag{4}$$

where $1/2$ is the normalization factor.

2.2. Lorentz gas with oscillating scatterer boundaries

Now we can easily obtain a mapping that describes the dynamics of a billiard with a perturbed boundary under the

assumption that the boundary oscillation amplitude is much smaller than its radius, i.e., we can neglect geometrical changes in its boundaries.

Suppose that the dispersing component ∂Q^+ of boundary ∂Q contracts and expands (Fig. 1), so that its radius varies following the law

$$R = R(t) = R + r(t), \quad \text{where} \quad \max|r(t)| \ll R.$$

Then the boundary velocity is a function of time, $u(t) = \dot{r}(t)$. Further, we assume for definiteness that $u(t) = u_0 \cos(\omega t)$, where $u_0 = \omega r_0$. In this case, in addition to parameters α and ϕ , we have to introduce another two variables, namely, the particle velocity v and collision time t . Given that only the normal (radial) component of the veloc-

ity changes in the process of scattering, and the tangential component remains unchanged, we obtain a mapping for the absolute value of particle velocity after the collision:

$$v_{n+1} = \sqrt{v_n^2 - 4u_n v_n \cos \alpha_n + 4u_n^2}. \quad (5)$$

Here $u_n \equiv u_0 \cos \omega t_n$ is the boundary velocity at the moment of the n th scattering event. The relation between the angles of incidence and reflection, in its turn, can be expressed as

$$\alpha_n^* = -\sin^{-1} \left(\frac{v_n}{v_{n+1}} \sin \alpha_n \right).$$

Now, by calculating the separation between sequential scattering events, one can easily obtain a mapping for the collision time t_n :

$$t_{n+1} = t_n + \frac{l_{n+1}}{v_{n+1}},$$

$$l_{n+1} = \sqrt{[R(\cos \phi_{n+1} - \cos \phi_n) - pa]^2 + [R(\sin \phi_{n+1} - \sin \phi_n) - qa]^2}. \quad (6)$$

Here l_n is the free path. Under the assumption that $r \ll R$, the mappings for variable ϕ and impact parameter d are the same as for the unperturbed billiard [Eqs. (1) and (2)].

3. FERMI ACCELERATION

As a result of impacts with a perturbed boundary, the billiard ball velocity always changes. As earlier research has shown,¹¹ these changes in the velocity are random. Therefore, let us consider an ensemble of particles and calculate their velocity distribution and average velocity as a function of time t and number of collisions n (the number of collisions and time are not directly proportional because a faster particle undergoes more impacts during a time interval than a slower one). In this section, we will first consider the issue of the mean change in the velocity in billiards with arbitrary shapes and perturbed boundaries, then we will discuss the problem of Fermi acceleration in a Lorentz gas with randomly and regularly oscillating scatterers.

3.1. Average change in the velocity in the general case

Consider two sequential collisions of a ball hitting against a wall in a billiard of an arbitrary configuration (Fig. 2). Denote by α_0 the particle incidence angle in the first collision, and by α_1 this angle in the second collision (they are introduced as in Sec. 2.1). Further, denote by v_0 and v_1 the absolute values of the ball velocity before the first and second collisions, respectively. The velocity components are labeled by the following indices: the superscripts τ and n denote the tangential and normal velocity components, respectively, the first subscript is the velocity index, the second is set to unity if the velocity component is considered before the collision and to zero after the collision. Thus, v_{10}^τ denotes the tangential component of velocity v_1 at the point of the first collision, and v_{11}^τ is the tangential component at the

point of the second collision. In the general case, they are not equal (Fig. 2). Let $u(t)$ be the boundary velocity. The following relation should, obviously, hold:

$$\langle u(t) \rangle_t = 0, \quad (7)$$

which means that the boundary remains, on average, at its place.

Consider a single collision between a particle and a wall. The tangential velocity component in this case is, obviously, constant, whereas the change in the normal component can be easily calculated in the reference frame connected to the wall. Thus, we can write for the first collision

$$v_{10}^n = -v_{01}^n + 2u(t_n) = -v_0 \cos \alpha_0 + 2u(t_n),$$

$$v_{10}^\tau = v_{01}^\tau = v_0 \sin \alpha_0, \quad (8)$$

$$v_1 = \sqrt{v_0^2 - 4v_{01}^n u(t_n) + 4u^2(t_n)}.$$

It is clear that, if only one collision is considered, $\langle \Delta v_{10}^\tau \rangle = 0$ and $\langle \Delta v_{10}^n \rangle = 0$ for a billiard of an arbitrary configuration. Moreover, changes in the velocity are associated only

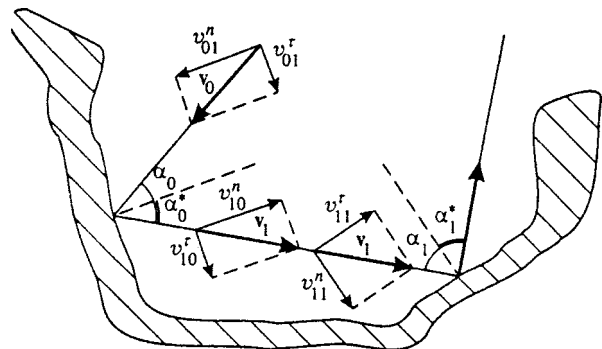


FIG. 2. Billiard of an arbitrary configuration.

with the normal component since the tangential component is unchanged after the reflection. Consequently, the average growth in the velocity depends on the normal velocity component in the next collision. In the general case, however, one can consider only the average velocity component, i.e.,

$$\begin{aligned} \langle v_{11}^n \rangle &= \langle v_1 \cos \alpha_1 \rangle \\ &= \langle \sqrt{v_0^2 - 4v_0 u(t) \cos \alpha_0 + 4u^2(t_n) \cos \alpha_1} \rangle, \end{aligned} \quad (9)$$

where averaging is performed over angles α_0 and α_1 and time t .

It seems appropriate to illustrate Eq. (9) on two examples.

Ulam's model.^{14,16–21} Two parallel heavy walls are placed at distance L between them, and a ball moves between these walls. One wall oscillates periodically with amplitude δ such that $L \gg \delta$. The specific time dependence of these oscillations is unimportant for our analysis, the only important point is that the wall motion should satisfy condition (7). Since the tangential velocity component in this model is constant, $v^t = \text{const}$, the velocity and incidence angle are related by the formula

$$v \sin \alpha = v^t = \text{const}. \quad (10)$$

The normal velocity component, in its turn, has the same absolute value before the first collision, v_{10}^n , and before the second, v_{11}^n . Consequently,

$$\langle v_{11}^n \rangle = \langle v_{10}^n \rangle = \langle -v_{01}^n + 2u(t_n) \rangle = v_{01}^n.$$

Thus, there is no particle acceleration on average in this model.

Lorentz gas. Owing to the strong mixing in this model, we can assume that angles α_0 and α_1 are mutually independent, hence

$$\langle v_{11}^n \rangle = \langle \cos \alpha_1 v_1 \rangle_{\alpha_0, \alpha_1, t} = \langle \cos \alpha_1 \rangle_{\alpha_1} \langle v_1 \rangle_{\alpha_0, t}.$$

Therefore, fluctuations in the velocity (increase and decrease) due to collisions are associated with changes in its absolute value, but not in its normal component, as was in the previous case. As will be shown below, the value $\langle v_n \rangle$ increases with n , therefore Fermi acceleration is feasible in the Lorentz gas.

This conclusion can probably be extended to other systems in which the incidence angle and velocity are not directly related by Eq. (10), as in Ulam's model. An intermediate configuration between Ulam's model and a scattering billiard is the "stadium-shaped" billiard, in which the feasibility of Fermi acceleration was studied numerically.¹¹

3.2. Stochastically perturbed scatterer boundary

Let the boundary velocity of a scatterer at which the n th collision takes place be

$$u_n(t) = u_0 \cos \varphi_n, \quad (11)$$

where u_0 is the boundary velocity amplitude, and $\{\varphi_n\}$ is a set of uncorrelated random values uniformly distributed over the interval $[0, 2\pi)$. Let us calculate the velocity distribution function and the average velocity in an ensemble of particles

as a function of the number n of scattering events and time t . In the case of a low particle velocity, $v \ll u_0$, the major contribution to velocity given by Eq. (5) is due to the last term on the right-hand side, hence

$$v_{n+1} \approx 2|u(t_n)|.$$

If boundary oscillations are determined by Eq. (11),

$$\langle v_{n+1} \rangle \approx 2 \langle |u(t_n)| \rangle_t = 4 \frac{u_0}{\pi}.$$

Thus, even after the first collision, the average velocity becomes larger than u_0 .

Now let us calculate the change in the velocity at $v \gg u_0$. By expanding the right-hand side of Eq. (5) in powers of u/v , we obtain an expression for the velocity change:

$$\begin{aligned} \Delta v_n = v_{n+1} - v_n &= -2u_n \cos \alpha_n + 2 \frac{u_n^2}{v_n} \\ &\times \sin^2 \alpha_n + v_n O\left(\left(\frac{u_n}{v_n}\right)^3\right), \end{aligned} \quad (12)$$

where u_n is the scatterer boundary velocity during the n th collision.

Using Eq. (4) and the uniformity of the phase distribution at the moment of collision, we obtain $\langle \Delta v_n \rangle$ and $\langle (\Delta v_n)^2 \rangle$:

$$\mu_s \equiv \langle \Delta v_n \rangle = \frac{M_s}{v}, \quad \sigma_s^2 \equiv \langle (\Delta v_n)^2 \rangle = \frac{4}{3} u_0^2. \quad (13)$$

Here we have introduced for simplicity of further calculations the parameter $M_s \equiv u_0^2/3$, where subscript s denotes the stochastic effect. After averaging, only the second term on the right of Eq. (12) contributes to the velocity increase, and in calculations of the variance the first term is sufficient.

If the number n of scattering events is sufficiently large, we can replace the first equation in (13) with a differential equation

$$\frac{\partial v(n)}{\partial n} = \frac{M_s}{v(n)}. \quad (14)$$

Its solution with the initial condition $v(0) = v_0$ yields the most probable velocity as a function of the number of collisions:

$$v(n) = \sqrt{2M_s n + v_0^2}. \quad (15)$$

Since the particle velocity is expressed as a sum of independent random quantities Δv_n with known mean and variance, it follows from Lyapunov's central limit theorem that the distribution function of the random value $v_n = v_0 + \sum_{i=1}^n \Delta v_i$ tends to a normal distribution with mean $v(n)$ and variance $n\sigma_s^2$. Thus, the velocity distribution has the shape of a spreading Gaussian. The position of the distribution peak is at the most probable velocity $v(n)$, proportional to the square root of n .

This reasoning applies only to the case of a sufficiently high particle velocity, $v \gg u_0$. In order to describe the distribution at lower velocities, let us introduce an additional condition, namely, that there is no flow of particles to the region

of negative velocities: $(v\partial\rho/\partial v)_{v=0}=0$. It is well known that the Gaussian distribution that satisfies this condition has the form

$$\rho(v, n) = \frac{1}{\sigma_s \sqrt{2\pi n}} \left[\exp\left(-\frac{[v - v(n)]^2}{2\sigma_s^2 n}\right) + \exp\left(-\frac{[v + v(n)]^2}{2\sigma_s^2 n}\right) \right]. \quad (16)$$

This allows us to calculate the mean velocity in the particle ensemble as a function of the number of scattering events:

$$V(n) = \sigma_s \sqrt{\frac{2n}{\pi}} \exp\left(-\frac{v^2(n)}{2\sigma_s^2 n}\right) + v(n) \Phi\left(\frac{v(n)}{\sigma_s \sqrt{2n}}\right), \quad (17)$$

where $\Phi(x) = (2/\sqrt{\pi}) \int_0^x \exp(-x^2) dx$ is the error function. Hereafter V denotes the mean velocity in the particle ensemble. By substituting all coefficients and expanding the expression for the velocity, we obtain

$$V(n) = C\sqrt{n} + O\left(\frac{1}{\sqrt{n}}\right), \quad (18)$$

where the constant $C = \sqrt{2}[\sigma_s \exp(-M_s/\sigma_s^2)/\sqrt{\pi} + \Phi(\sqrt{M_s}/\sigma_s)/\sqrt{M_s}] \approx 1.143u_0$.

Thus, Eqs. (16) and (18) determine the velocity distribution and the mean velocity in the ensemble as functions of the number of scattering events.

To calculate the mean velocity versus time we use the Fokker-Planck equation:

$$\frac{\partial\rho(v, t)}{\partial t} = -\frac{\partial}{\partial v}[A\rho(v, t)] + \frac{1}{2} \frac{\partial^2}{\partial v^2}[B\rho(v, t)],$$

where the factors A and B are given by the expressions

$$A \equiv \left\langle \frac{\Delta v}{\tau} \right\rangle = \frac{M_s}{l}, \quad B \equiv \left\langle \frac{\Delta v^2}{\tau} \right\rangle = \frac{\sigma_s^2 v}{l}.$$

Here the mean time between collisions $\tau = l/v$, l is the mean free path, and Δv and Δv^2 are defined by Eq. (13). By substituting the resulting coefficients in the equation, we obtain

$$\frac{\partial\rho(v, t)}{\partial t} = -\frac{M_s}{l} \frac{\partial}{\partial v}\rho(v, t) + \frac{1}{2} \frac{\sigma_s^2}{l} \frac{\partial^2}{\partial v^2}[v\rho(v, t)]. \quad (19)$$

If parameters M_s and σ_s are determined in accordance with Eq. (13), the solution of this equation in the limit of high velocities much larger than the initial value, i.e., after a sufficiently long time interval, tends to

$$\rho(v, t) = \frac{1}{\sqrt{2tA\pi v}} \exp\left(-\frac{v}{2tA}\right),$$

where $A = M_s/l$. The latter expression yields the mean particle velocity:

$$V(t) = \frac{M_s}{l} t + v_0 = \frac{1}{3} \frac{u_0^2}{l} t + v_0. \quad (20)$$

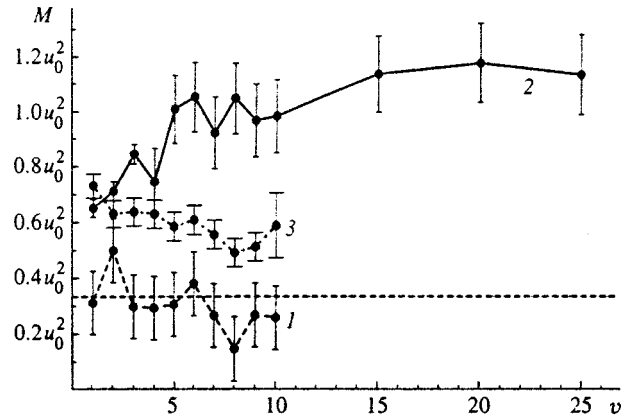


FIG. 3. Parameter $M \equiv v\langle\Delta v\rangle$ as a function of particle velocity. Curves 1 and 2 are calculated by the Lorentz gas model for the cases of random and regular boundary oscillations, respectively. Curve 3 is calculated using the simplified mapping (22). The dashed line shows M_s in the Lorentz gas in the case of stochastic boundary oscillations calculated by Eq. (13). Results are obtained at $u_0=0.01$, $a=1$, and $R=0.4$.

Thus, the system under investigation gives rise to the Fermi acceleration, with the particle velocity increasing as a linear function of time.

3.3. Periodically perturbed scatterer boundaries

Suppose that all scatterer boundaries contract and expand following a certain periodic law with a constant initial phase. Then, during one half of the period, the particle velocity should increase as a result of collisions and decrease during the other half. If the particle velocity is high enough, the time τ_s between scattering events is longer than the period T of scatterer oscillations. This leads to correlations in particle velocity variations, so the sequential increments in the velocity defined by Eq. (12) can no longer be treated as independent.

This section presents numerical calculations of the velocity variance and its average increase, alongside the decay rate of the correlation function $R(m) = \langle\Delta v_n \Delta v_{n+m}\rangle$. They indicate, in particular, that correlations can lead to larger first and second moments of velocity distributions. The calculations were performed on the basis of the Lorentz gas model with the following parameters: the scatterer radius $R=0.4$; the separation between their centers $a=1$ [thus, the basic model parameter $(a/R)^2=6.25$]; the amplitude of the scatterer surface velocity $u_0=0.01$; the oscillation frequency $\omega=1$.

It follows from the analysis of the previous subsection that at high particle velocities $\langle\Delta v\rangle \sim 1/v$. Therefore, the variable most convenient for the analysis and graphic representation is $M \equiv \langle\Delta v\rangle v$. Figure 3 shows M plotted against the particle velocity in the case of stochastic (curve 1) and periodic (curve 2) boundary oscillations. One can see that, in the case of stochastic oscillations, the variable $M_s \approx u_0^2/3$ coincides with the result of the previous subsection. In the case of regular oscillations, M_r first increases, and then most likely tends to a constant $M_r^{\max} = (1.15 \pm 0.10)u_0^2$ at $v \geq 15$, which corresponds in this specific billiard configuration to $n \geq 150$ particle collisions with the boundary during one os-

cillation period on average. In addition, it is clear that the particle acceleration in the case of regular boundary oscillations is a factor of three to four higher than in the case of stochastic oscillations.

For the analysis of velocity changes in chaotic billiards with periodically oscillating boundaries, the following approach can be suggested. Consider an approximate mapping for velocity (12). Since correlations between parameters α_n decay exponentially (as follows from the billiard configuration), the formulas can be averaged over α using Eq. (4). Then

$$\langle \Delta v \rangle_\alpha = -\frac{\pi}{2} u_0 \cos \omega t_n + \frac{u_0^2 \cos \omega t_n}{v_n}. \quad (21)$$

During the oscillation period, the largest contribution to changes in the velocity is due to the first term on the right. Therefore, it is sufficient in the first approximation to take into account only the changes in the velocity due to the first term, and the second can be neglected. On the other hand, correlational corrections to the second term generate terms of higher orders than that of its average. Therefore, correlation effects in the second term can be neglected. For this reason, the two values related to the first and second terms can be calculated independently:

$$\langle \Delta v \rangle = \langle \Delta v \rangle_I + \langle \Delta v \rangle_{II},$$

where $\langle v \rangle_{II} = u_0^2 / (3v)$, which coincides with μ_s in the stochastic case [Eq. (13)], and $\langle \Delta v \rangle_I$ is the correction due to correlations. Discarding the second term on the right of Eq. (21), we have the following mapping for calculating $\langle \Delta v \rangle_I$:

$$v_{n+1} = v_n + \gamma \cos \theta_n, \quad \theta_{n+1} = \theta_n + \frac{l_{n+1} \omega}{v_{n+1}}. \quad (22)$$

Here $\gamma = -\pi u_0 / 2$, and the collision phase $\theta_n \equiv \omega t_n$ is substituted for time. This mapping is exactly equivalent to Ulam's well-known mapping,¹⁴⁻²¹ the only difference being that in this case the free path l_n is a random parameter distributed over a certain interval.

Let us analyze numerically this mapping at the same values of u_0 and ω as those selected in our analysis of the Lorentz gas. Suppose that the free path l_n has a normal distribution with mean $l = 0.62$ and variance $\sigma_l^2 = 0.657$. This corresponds to the variance and mean free path calculated numerically at $R = 0.4$ and $a = 1$ (see the previous subsection). Figure 3 shows $\langle \Delta v \rangle_I v + u_0^2 / 3$ (curve 3) derived from mapping (22). One can see in the graph that the first moment of the velocity distribution defined by this mapping becomes positive, but it is still smaller than the observed velocity increase in the Lorentz gas. Nonetheless, this mapping is easier for analysis than Eq. (21).

Now let us estimate the variance and decay rate of correlations in the velocity change. Suppose that the particle velocity is so high that its change after n scattering events is negligible. It is clear that, in order to satisfy this condition, one can choose v and u_0 in a proper manner. Let us calculate correlations between velocity increments Δv_m and Δv_{m+n} [Eq. (12)] for $n \rightarrow \infty$. Taking into account in the first approximation only the first terms on the right of Eq. (12), we obtain

$$R(n) \equiv \langle \Delta v_m \Delta v_{m+n} \rangle = u_0^2 \frac{\pi^2}{4} \langle \cos \omega t_m \cos \omega t_{m+n} \rangle,$$

which takes into account, as follows from Eq. (4), that $\langle \cos \alpha_n \rangle = \pi/4$. By setting the oscillation frequency to unity and introducing the notation $S_n \equiv \sum_{i=1}^n \tau_{m+i}$, where $\tau_i = t_i - t_{i-1}$, we obtain

$$\langle \cos t_m \cos t_{m+n} \rangle = \langle \cos t_m \cos(t_m + S_n) \rangle.$$

The variable S_n can be expressed as

$$S_n = \sum_{i=1}^n (l + \Delta l_i) / v,$$

where Δl_i is the deviation from the mean free path on the i th collision. Since S_n is the sum of independent random quantities, its distribution at large n tends to the normal distribution with mean nl and variance $n\sigma_l^2$, where σ_l^2 is the mean free path variance. By expanding the cosine of the sum and averaging over S_n , we obtain the following expression for the correlation function of velocity increments:

$$R(n) \approx \frac{\pi^2}{8} u_0^2 \cos(\omega n \tau) \exp\left(-\frac{n}{N}\right), \quad (23)$$

where ω is the frequency of scatterer oscillations, $N = v^2 / (\omega^2 \sigma_l^2)$. Thus, correlations between sequential changes in the particle velocity are the stronger, the higher the velocity, and their "half-life" N , i.e., the number of collisions after which correlations drop by factor e , increases proportionally to v^2 . Note that the number of collisions over one period is proportional to v . Thus, in order to estimate correctly the velocity variance, one has to average over the larger number of oscillation periods, the higher the particle velocity. The issue of how this can be done, however, has remained unresolved.

In order to estimate the variance in the first approximation, let us consider the velocity increment after two sequential collisions with the boundary. In this analysis, we assume that correlations among three and more increments are negligible. In the limit of a high velocity of a billiard particle, the correlator of sequential velocity increments can be estimated by the formula

$$\begin{aligned} \langle \Delta v_n \Delta v_{n+1} \rangle &= u_0^2 \frac{\pi^2}{4} \langle \cos^2 \omega t_n (1 - O(\tau^2)) \rangle \\ &= u_0^2 \frac{\pi^2}{8} + O\left(\frac{u_0^2}{v^2}\right). \end{aligned}$$

From this expression and Eq. (13), we derive

$$\sigma_r^2 = \frac{\langle (\Delta v_n + \Delta v_{n+1})^2 \rangle}{2} \approx \left(\frac{4}{3} + \frac{\pi^2}{8}\right) u_0^2. \quad (24)$$

Figure 4 shows numerical and analytic estimates of the velocity increment variance in the stochastic (dashed line) and regular (solid lines) cases. In the case of stochastic oscillations, the numerical and analytic [Eq. (13)] estimates are identical, so the graph shows only numerical calculations of σ_s^2 . Regular oscillations are characterized in this graph by the straight line defined by Eq. (24) and the broken line

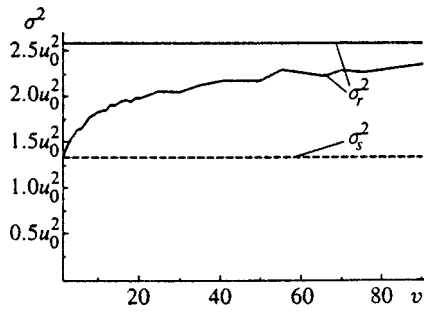


FIG. 4. Variance versus particle velocity in the Lorentz gas in the cases of stochastic (dashed line) and regular (solid lines) oscillations. The straight line shows the theoretical estimate of the variance in the regular case by Eq. (24). The calculations were performed at $u_0=0.01$, $a=1$, and $R=0.4$.

calculated numerically. In order to take into account correlations between velocity increments, we calculated in the regular case the effective variance $\sigma_r^2 = \langle \Delta V^2 \rangle / N_{\max}$, where ΔV is the total velocity increment after N_{\max} collisions. Given Eq. (23) describing the correlation function decay, we equated N_{\max} to $10v^2/(\omega^2\sigma_l^2)$, which is a factor of ten higher than the characteristic correlation decoupling number. As is shown by the graphs, the variance σ_s^2 in the stochastic case is constant, whereas in the regular case (σ_r^2) it grows with the velocity. In addition, the variance in the regular case determined by Eq. (24) is slightly overestimated.

Thus, the numerical and analytic estimates given in this section indicate that particle acceleration should occur in chaotic billiards with periodically oscillating boundaries. We can most likely say that deterministic chaoticity is a sufficient condition for Fermi acceleration. Moreover, periodic oscillations of billiard boundaries lead to a higher particle acceleration.

3.4. Numerical results

This section presents numerically calculated particle velocity as a function of the number of scattering events and time in comparison with the analytic estimates given above. The calculations were performed by the Lorentz gas model with the following parameters: the amplitude of the scatterer boundary oscillation velocity $u_0=0.01$; the scatterer radius $R=0.4$; the distance between their centers $a=1$; the frequency of boundary oscillations $\omega=1$; the initial velocity $v_0=1$. Thus, the mean free path calculated analytically for these parameters, $l=0.6216815$. The numerical calculations of the mean free path [Eq. (6)] and its variance in this specific billiard configuration yield $l=0.62163 \pm 0.00003$ and $\sigma_l^2=0.657 \pm 0.001$.

The difference in realizations was in the initial values of α and ϕ , which were selected at random. Two different cases were investigated: stochastic oscillations of scatterer boundaries with initial phases distributed uniformly and regular oscillations of boundaries. In both cases, the billiard ball (particle) dynamics was determined by the mapping derived in Secs. 2.1 and 2.2. The scatterer boundary oscillation velocity in the first case was defined by the formula

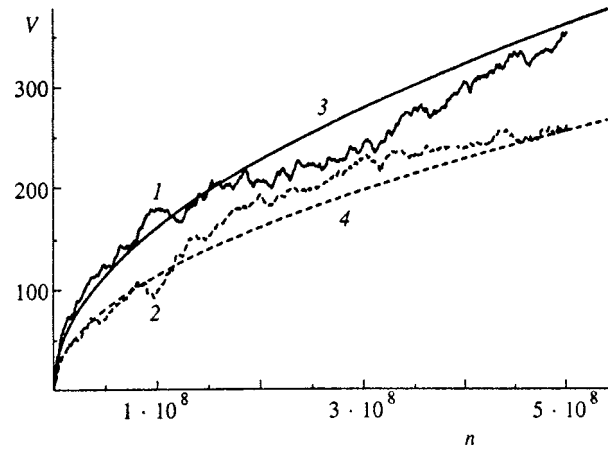


FIG. 5. Mean particle velocities as functions of the number of scattering events in the Lorentz gas (curves 1 and 2) and their approximations by Eq. (18) (curves 3 and 4). The dashed lines correspond to stochastic boundary oscillations, the solid lines correspond to regular oscillations. The averaging was performed over 100 process realizations with different velocity directions selected at random. The calculation were performed at $u_0=0.01$, $a=1$, and $R=0.4$.

$u_n = u_0 \cos \varphi_n$, where φ_n is a random parameter uniformly distributed over the interval $[0, 2\pi)$, and in the second case by the formula $u_n = u_0 \cos \omega t_n$, where t_n is the moment of collision between the particle and boundary. For each case 100 realizations of billiard dynamics were investigated. The averaged velocity as a function of the number of scattering events and time is plotted in Figs. 5 and 6, respectively. In both graphs, the solid lines plot the data for the regular case, and the dashed line corresponds to the case of random oscillations.

Figure 5 shows the averaged velocity of an ensemble of particles versus the number n of scattering events over the range of 5×10^8 iterations. It is clear that both curves are accurately approximated by the square-root function (18). In the case of stochastic oscillations, parameters M_s and σ_s were derived from Eq. (13), and in the regular case the limiting values M_r and σ_r were derived from numerical calculations described in the previous subsection.

The curves of the mean velocity versus time (Fig. 6) plot the data averaged over 100 realizations in the stochastic (dashed lines) and regular (solid lines) cases. The particle dynamics was simulated over a time interval of $[0, 3 \times 10^6]$ time units, and some trajectories of ‘‘fast’’ particles covered up to 3×10^9 iterations. The mean particle velocity was approximated using Eq. (20). The parameter M_s was calculated for stochastic oscillations by Eq. (13), and for regular oscillations as a limit of M_r obtained in the previous subsection. The curves show that the growth in the particle velocity is approximately linear, and the approximation of the average velocity by Eq. (20) is in reasonable agreement with computer simulations.

4. CONCLUSIONS

Billiards are fairly convenient models of a set of physical systems. For example, particle trajectories in billiards of specific configurations can be used in modeling many dy-

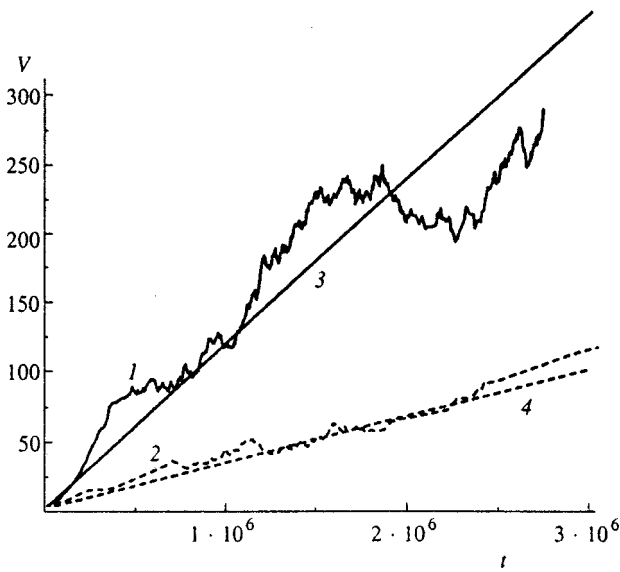


FIG. 6. The same data as in Fig. 5, but plotted against time. The approximation was performed by Eq. (20).

namical systems. Moreover, most approaches to the problems of mixing in many-body systems originate from billiard-like problems. A natural generalization of a billiard system is a billiard whose boundary is not fixed, but varies following a certain law. This is a relatively new field of research, which opens new prospects in studies of problems that have been known for a long time, but have been poorly investigated. For example, the problem of particle dynamics in a billiard whose boundary changes with time has a direct physical application as a model of nonequilibrium statistical mechanics. As follows from the existing literature, the dynamical properties of a billiard with perturbed boundaries are important: if its dynamics is chaotic, boundary perturbations can lead to an infinite growth in the particle velocity, i.e., such a billiard demonstrates Fermi acceleration.

In the present article, we have studied the problem of Fermi acceleration in dynamical systems generated by two-dimensional dispersing billiards with perturbed boundaries. A billiard with a boundary like that of the Lorentz gas oscillating in accordance with a certain law has been investigated. It is well known that the conventional Lorentz gas (i.e., that with an unperturbed boundary) has clearly demonstrated chaotic properties (mixing, decay of correlations, etc.). Perturbation of boundaries in such a billiard leads to the Fermi acceleration. This model has been studied in two versions, namely, those with stochastically and regularly oscillating scatterer boundaries. It has turned out that the acceleration is higher in the case of periodical boundary oscillations.

We can identify two basic acceleration mechanisms, which have been discovered in deriving the particle velocity distribution as a function of the number of scattering events in the case of stochastic oscillations (Sec. 3.3). The first is the mechanism deriving from the condition $\langle \Delta v \rangle > 0$ [Eq. (13)], which drives all particles to the side of higher velocities. The second is the dispersive (or fluctuational) mechanism controlled by two conditions: (a) $\langle \Delta v^2 \rangle > 0$, therefore

the peak in the velocity distribution spreads with time; (b) the absolute value of velocity cannot be negative, therefore the peak spread cannot be symmetrical, but its predominant direction is to the side of higher velocities, as a result, the simple normal distribution is replaced by distribution (16). Moreover, it follows from both analytic and numerical calculations that fluctuations and the mean increase in the particle velocity are larger in the case of regular scatterer boundary oscillations, which leads to a larger velocity growth. Thus, the mechanism due to correlations between sequential changes in the velocity has been suggested.

It is quite clear that the reasoning used in deriving the particle velocity as a function of the number of scattering events and time can be directly translated into another type of billiard in which a distribution of angle α (between the normal to the surface at the impact point and particle velocity) is known. Therefore, the technique developed in our work can be used in solving the problem of Fermi acceleration in the general case.

The presence of a chaotic condition in a system can change its statistical properties. A recent publication by Tsang and Ngai¹⁰ considered a billiard in an area defined by a rectangle whose corners were replaced by quarter-circles of radius R (smoothed corners) and one side oscillated periodically. A particle travels within this area and collides with the boundaries. Each collision with the boundary is not perfectly elastic, and the particle loses a fraction of its energy proportional to a constant δ ($\delta \ll 1$). This model is similar to Ulam's model, but the presence of smoothed corners introduces random elements to the particle dynamics. Tsang and Ngai¹⁰ investigated relaxation of a system to equilibrium. A similar investigation was performed earlier by Tsang and Lieberman²⁵ on the basis of Ulam's model. It was shown that the function $\Phi(t) = E(t) - E(\infty)$, which is the deviation of the mean energy from the equilibrium value, drops exponentially, $\Phi(t) \propto \exp(-t/\tau)$, which is quite natural of most physical systems. The investigation of this parameter in the billiard discussed in Ref. 10 revealed that its relaxation to equilibrium in this case is slower, $\Phi(t) \propto \exp[-(t/\tau)^\beta]$, where $\beta < 1$ and drops with R . Given the results of this paper, we can understand the cause of the slower system relaxation. In fact, the random element in the system becomes more important at larger radii of circles at the corners, which leads to acceleration of particles. Therefore the system relaxation to its equilibrium, associated with the particle energy dissipation in the system, becomes slower. The approaches developed in the reported work create preconditions for determination of β , hence of the relaxation rate to equilibrium in a system where the chaotic dynamics is dominant.

Thus, on the basis of our investigations, we can put forth an important hypothesis: a random element in a billiard with a fixed boundary is a sufficient condition for the Fermi acceleration in the system when a boundary perturbation is introduced.

*E-mail: loskutov@moldyn.phys.msu.su

- ¹Ya. G. Sinai, *Usp. Mat. Nauk* **25**, 141 (1970).
²L. A. Bunimovich, *Commun. Math. Phys.* **65**, 295 (1979).
³L. A. Bunimovich and Ya. G. Sinai, *Commun. Math. Phys.* **78**, 479 (1981).
⁴L. A. Bunimovich, *Dynamical Systems*, Vol. 2 [in Russian], VINITI, Moscow (1985), p. 173.
⁵L. A. Bunimovich, *Chaos* **1**, 187 (1991).
⁶A. Tabachnikov, *Billiards*, France Math. Soc. Press, Lyon (1995).
⁷*Proc. of the Int. Conf. on Classical and Quantum Billiards*, *J. Stat. Phys.* **83** (1–2) (1996).
⁸J. Koiller, R. Markarian, S.Q. Kamphorst, and S. P. de Carvalho, *Nonlinearity* **8**, 983 (1995); *J. Stat. Phys.* **83**, 127 (1996).
⁹*New Trends in Hamiltonian Systems*, World Scientific, Singapore (1996).
¹⁰K. J. Tsang and K. L. Ngai, *Phys. Rev. E* **56**, R17 (1997).
¹¹L. G. Akinshin, K. A. Vasil'ev, A. Yu. Loskutov, and A. B. Ryabov, *Physical Ideas of Russia* [in Russian] **2–3**, 87 (1997).
¹²E. Fermi, *Phys. Rev.* **75**, 1169 (1949).
¹³G. M. Zaslavskii and B. V. Chirikov, *Dokl. Akad. Nauk SSSR* **159**, 306 (1964) [*Sov. Phys. Doklady* **9**, 989 (1964)].
¹⁴S. M. Ulam, in *Proc. of the 4th Berkeley Symp. on Math. Stat. and Probability*, California Univ. Press (1961), Vol. 3, p. 315.
¹⁵A. Brahic, *Astron. Astrophys.* **12**, 98 (1971).
¹⁶A. J. Lichtenberg and M. A. Lieberman, *Regular and Chaotic Dynamics*, Springer-Verlag, New York (1992).
¹⁷G. M. Zaslavskii, *Stochastic Irreversibility in Nonlinear Systems* [in Russian], Nauka, Moscow (1970).
¹⁸A. J. Lichtenberg, M. A. Lieberman, and R. H. Cohen, *Physica D* **1**, 291 (1980).
¹⁹L. D. Pustyl'nikov, *Dokl. Akad. Nauk SSSR* **292**, 549 (1987) [*sic*].
²⁰L. D. Pustyl'nikov, *Mat. Sb.* **85**, 113 (1994).
²¹T. Krüger, L. D. Pustyl'nikov, and S. E. Troubetzkoy, *Nonlinearity* **8**, 397 (1995).
²²P. R. Baldwin, *J. Phys. A* **24**, L941 (1991).
²³N. Chernov, *J. Stat. Phys.* **88**, 1 (1997).
²⁴P. L. Garrido, *J. Stat. Phys.* **88**, 807 (1997).
²⁵K. J. Tsang and M. A. Lieberman, *Physica D* **11**, 147 (1984); *Phys. Lett. A* **103**, 175 (1984).

Translation provided by the Russian Editorial office